energies

MDPI

Article

Standardized Comparison of 40 Local Driving Cycles: Energy and Kinematics

Guilherme Medeiros Soares de Andrade, Fernando Wesley Cavalcanti de Araújo, Maurício Pereira Magalhães de Novaes Santos and Fabio Santana Magnani *

Center of Technologies and Geosciences, Department of Mechanical Engineering, Federal University of Pernambuco, Recife 50740-550, Brazil; guilherme.soaresandrade@ufpe.br (G.M.S.d.A.); fernando.wesley@ufpe.br (F.W.C.d.A.); mauricio.novaessantos@ufpe.br (M.P.M.d.N.S.)

* Correspondence: fabio.magnani@ufpe.br

Received: 17 August 2020; Accepted: 14 October 2020; Published: 18 October 2020

Abstract: Local driving cycles (LDCs) capture local traffic characteristics, while standard driving cycles (SDCs) compare vehicles in distinct regions. There is a plethora of LDCs, raising the question as to how distinct they are. To quantify it, we first organized a collection of 77 LDCs. From the speed—time images, it was possible to extract numerical vectors of 40 cycles in a standardized way. Comparing the LDCs developed for cars, we found that their parameters fluctuate significantly: the average speed varies from 14.7 to 44.7 km/h, and the fuel economy varies from 10.8 to 20.5 km/L. Comparing the LDCs with FTP-75 cycle, the difference in speed is 7 km/h, and in fuel economy is 1.5 km/L. For WLTC, the difference is 19.4 km/h and 3 km/L, respectively. Thus, given the deviations found between the analyzed LDCs, and between LDCs and SDCs, the numerical results reinforce the relevance of using LDCs for each region.

Keywords: fuel economy; characteristic parameters; driving cycles; energy consumption; average speed

1. Introduction

A driving cycle (DCs) is a time–speed series that represents a driving pattern to depict a real-world behavior [1]. Government, researchers, and manufacturers use standard driving cycles (SDCs) to estimate emission and consumption [2,3]. The DCs are used for several purposes, for example: vehicle design (e.g., evaluating the impact of modifying vehicle parts, engine calibration, aerodynamics, choice of tires in the emission, fuel consumption, and drivability), optimization and assessment of new technologies (e.g., the energy management system of hybrid vehicles [4–7]), and evaluation of emission levels as required by the legislation (e.g., European emission standards (Euro) and Brazilian emission standards (PROCONVE)). Examples of the most employed SDCs are FTP-75 cycle (USA), JC08 (Japan), NEDC, and WLTC (Europe). Despite all of the efforts to generate a SDC that considers average real-world driving, there is a growing concern regarding the differences in the results obtained from the type approval tests and those under real-world conditions, because the difference can be up to 60% [8].

This difference between the results can be assigned to several factors, such as the vehicle's characteristic (e.g., vehicle age and mileage, fuel employed, vehicle shape), traffic conditions, road, driver behavior, and the procedure applied to evaluate the vehicle energy consumption. In order to better estimate the actual energy usage of the vehicles in the real-world, new type approval tests are developed, which usually include new driving cycles to be used in laboratory tests, and new procedures (e.g., certification test initial temperature, gear changing criteria, tire calibration, usage of auxiliary equipment) [9]. Besides using stricter procedures, the values obtained in the certification test can be adjusted, applying a correction factor [10].

Another approach employed from researchers to minimize the difference for energy consumption and emission is replacing SDCs for local driving cycles (LDCs). Each LDC attempts to provide values representative of the region in which they are assessed. Several researchers developed LDCs; thus, there are numerous cycles with different characteristics available in the literature [11]. One approach to compare LDCs and SDCs is by evaluating their characteristic kinematic parameters (CPs) [8], such as average speed and average acceleration. They can also be compared using energy parameters (EPs).

In past decades, several LDCs have been published around the world. This compels the research question on how much LDCs differ numerically among themselves, and between themselves and the SDCs. In this context, the main objective of this work is to numerically compare the differences between the various LDCs among themselves, as well compare the differences between LDCs and SDCs. Those differences are calculated in function of the CPs, fuel economy (FE), and energy consumption (EC).

1.1. Comparison of Kinematic and Energy Parameters of Driving Cycles

Several papers also present comparisons between cycles (LDCs or SDCs). In Section 3.1, we will present a list of the 77 LDCs developed from 1978 to 2020 for cities in Asia, Europe, Oceania, and South and North America. To briefly exemplify the differences between the cycles, we now present some of the results in the literature comparing the average speed (V), the average acceleration (a), and the idling time percentage (IT). Arun et al. [12] generated LDCs for cars in Chennai (India), finding differences between peak and off-peak hours (ΔV = 4.4 km/h, Δa = 0.16 m/s^2, ΔIT = 15%), as well as when compared with FTP-75 cycle (ΔV = 14.2 km/h, Δa = 0.08 m/s^2, ΔIT = 12%). Tong et al. [13] proposed an LDC for Hanoi (Vietnam), concluding that there was a difference between their cycle and the standard cycle used at the time, NEDC (ΔV = 13.7 km/h, Δa = 0.13 m/s^2, ΔIT = 15%). Knez et al. [14] compared previous cycles to their proposed driving cycle for Celje (Slovenia), observing that small towns have higher average speed (ΔV = 6.1 km/h, Δa = 0.17 m/s^2, ΔIT = 5%). Mayakuntla and Verma [11] developed a driving cycle for Bangalore (India), finding that different regions in India need different cycles (ΔV = 2.3 km/h, ΔIT = 13% in their comparison). They also emphasized the need to abandon the SDC used for legislative purposes in favor of LDCs (they found ΔV = 10.7 km/h, Δa = 0.93 m/s^2, and ΔIT = 6% when comparing their LDC with an SDC).

A remarkable review of driving cycles was performed by Barlow et al. [15], presenting CPs for 256 worldwide driving cycles. It is an important document that provides the mathematical definitions of the most relevant CPs and allows their comparison in numerous cycles, both legislated (e.g., FTP-75 cycle, WLTC, and WMTC) and non-legislated (e.g., as ARTEMIS, INRET, and OSCAR), as categorized by [16].

In additional to studying the CPs for the driving cycles, some authors also evaluated EPs (e.g., EC and FE). Approximately one third of the papers listed in Section 3.1 evaluate energy. Tsai et al. [17] found the energy consumption of the Kaohsiung driving cycle is approximately 10% higher than that of the ECE (an European standard cycle). In Chen et al. [18], the fuel economy of the urban driving cycle is 21% lower than the rural driving cycle in Taiwan. Ho et al. [19] calculated that the energy consumption of the NEDC is 5% lower than the Singapore driving cycle. In Karavalakis et al. [20], the energy consumption increased approximately 30% in comparison to the NEDC. Roso and Martins [21] estimated that the energy consumption of the Santa Maria driving cycle at 12 a.m. and at 5 p.m. is smaller than the FTP-75 cycle by 1.5% and 21%, respectively. In Ma et al. [2], the energy consumption of the Beijing peak and off-peak cycles are higher than the NEDC by 37.5% and 29.3%, respectively. Other papers also analyzed energy parameters, as Tzeng and Chen [22], Azevedo et al. [23], Gong et al. [24], Koossalapeerom et al. [25], and Rechkemmer et al. [26]. It should be considered that there are different approaches used to calculate the energy usage, such as: dynamometer test [5,17,18,20,22], computer simulation (e.g., GT-Suite [21], Autonomie [4], and ADVISOR [6,7]), instantaneous vehicle fuel consumption modeling [2,19,26], and energy measurements performed with onboard equipment in on-road driving experiments [23–25].

1.2. Contribution of the Study

The main contribution of this study is the quantification of the kinematic and energy differences among the various LDCs, as well as the quantification of the differences between the LDCs and the SDCs. Other contributions of this work are an organized list with 77 LDCs surveyed from the literature; a homogenized list (i.e., the parameters are now calculated using the same methodology) with 40 LDCs (the data could not be obtained from the other 37 cycles); an in-depth energy analysis studying how the energy is used to overcome each one of the resistances (i.e., aerodynamic drag, inertia, rolling, and idling); and a study on the influence of the kinematic parameters of the cycles on the fuel economy of the vehicles.

2. Methodology

This section comprises three subtopics: extraction of the numerical vectors from the speed—time profile figures, characterization of the cycles in terms of the CPs, and computer simulation of the EPs.

2.1. Data Selection, Extraction, and Filtering

We first performed a detailed bibliographic search to determine which LDCs could be used. To be selected, a paper should have presented at least a figure containing the speed—time profile, provided access to the full text (some congress papers are difficult to find), and proposed at least one new LDC. Using this method, we collected 77 LDCs from 32 papers. Some authors developed more than one LDC in their studies. Examples are Lai et al. [27], who developed 9 driving cycles for buses in Beijing, and Amirjamshidi and Roorda [1], who constructed 15 driving cycles for trucks in Toronto, Canada. For reference and validation, we used two SDCs: FTP-75 cycle and WLTC.

To obtain the numerical vectors from the speed—time profiles, we requested for the data for all the LDCs listed in this paper, thus, obtaining the data from three authors who shared one or more LDCs [1,12,20]. The majority of the requested emails returned because of discontinued electronic addresses or information technology problems. Selph et al. [28] discuss how the response rate for online requests is usually low. Therefore, to obtain the numerical vectors from the speed–time profiles, we employed the publicly available web-based software, WebPlotDigitizer, to automatically extract numerical data from the figures. This method is considered to be accurate and efficient [29,30]. However, factors, such as image resolution, line color, thickness, and presence of other data in the figure, influence the final results.

Figure 1 presents a time section of the original FTP-75 cycle data and the corresponding extracted data. It can verify that the extraction is highly adequate, with the exception of sparse points, in which case the data for speed (V) are not perfectly extracted at specific times (t) (e.g., V = 0 at t = 727 s, t = 766 s, and t = 957 s). It is identified that, it is possible to manually edit the points extracted by the software (i.e., adding, removing, or adjusting). However, we preferred to use an automatic extraction process for all the LDCs, intending to employ the least human intervention. The validation will −demonstrate this procedure is numerically reasonable.

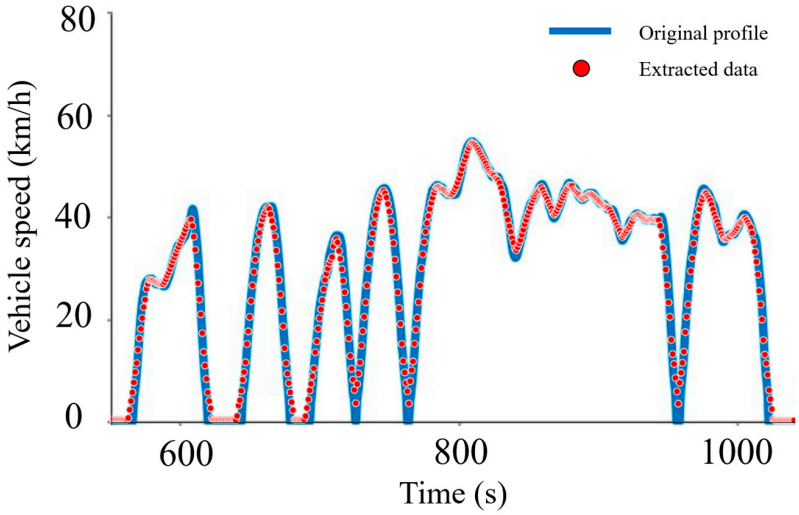

Figure 1. Example of data extraction in WebPlotDigitizer for a time section in FTP-75 cycle.

We noticed the extraction method generated noise in certain cases: low-speed numerical noise when it should be null, unreal speed fluctuations when the speed should be constant, and unrealistic accelerations. To correct those anomalies, we filtered the raw data from WebPlotDigitizer using the set of conditions listed in Table 1.

Table 1. Conditions in the filtering process.

Condition (If)	Result (Then)	Reason
$V < 3.6$ km/h	$V = 0$ km/h	Provide null speed (Idling mode)
$a < 0.05$ m/s^2	$a = 0$ m/s^2	Avoid acceleration fluctuation (Cruising mode)
$d < -0.05$ m/s^2	$d = 0$ m/s^2	Avoid deceleration fluctuation (Cruising mode)
$a > 3$ m/s^2	$a = 3$ m/s^2	Limit maximum acceleration
$d < -7$ m/s^2	$d = -7$ m/s^2	Limit maximum deceleration

Not all of the figures were adequately extracted, as easily confirmed by a visual inspection. From the 77 LDCs collected in the study, 40 generated good numerical vectors following the extraction process (Section 3.3). The other 37 could not be considered. For example, Figure 2 presents two LDCs whose data could not be adequately extracted (in contrast to Figure 1, which presents a successful extraction example). The software was unable to extract the data precisely for Celje and Shanghai because of the line thickness.

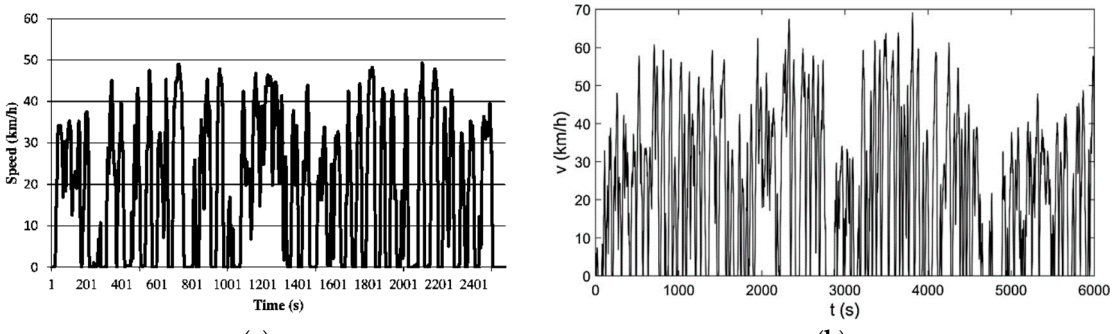

(**a**) (**b**)

Figure 2. Examples of local driving cycles (LDCs) that could not be adequately extracted: (**a**) Celje [14] (Reprint with permission [4930310296243]; Copyright Year 2020, Publisher: Elsevier) and (**b**) Shanghai [31] (Reprint with permission [4930290354283]; Copyright Year 2020, Publisher: Elsevier).

2.2. Evaluating Characteristic Parameters

Each author uses a specific set of parameters to evaluate the CPs in his/her research. For example, consider the CP, "time spent accelerating." Chen et al. [18], Tong et al. [32], and Wang et al. [33] considered that a vehicle is accelerating when $a > 0.1$ m/s^2; Amirjamshidi and Roorda [1] and Arun et al. [12] required two combined conditions, when $V > 5$ km/h and $a > 0.1$ m/s^2. Koossalapeerom et al. [25] and Ma et al. [2] considered the fractions of time to reach $a \geq 0.27$ m/s^2 and $a > 0.28$ m/s^2, respectively. In this study, to compare the LDCs, we use the same set of parameters to characterize all of the driving cycles, as defined in Table 2. It is important to emphasize that the parameters listed in Table 2 should be used only subsequent to the filtering process described in Table 1.

Table 2. Parameters for the characterization process—to be used following the filtering process described in.

Characteristic Parameters	Symbol	Definition
Average speed	V (km/h)	Average speed including zero speed
Distance	D (km)	Distance traveled
Average acceleration	a (m/s^2)	Average acceleration rate above 0.0 m/s^2
Average deceleration	d (m/s^2)	Average deceleration rate below 0.0 m/s^2
Time	t (s)	Total test time
Idling mode	IT (%)	Time proportion in which V = 0.0 km/h and a = 0.0 m/s^2
Acceleration mode	AT (%)	Time proportion in which $a > 0.0$ m/s^2
Deceleration mode	DT (%)	Time proportion in which $a < 0.0$ m/s^2
Cruising mode	CT (%)	100%—IT—AT—DT

2.3. Evaluating the Energy Parameters

In Section 2.2, we described the standardized process to obtain the numerical vectors from the speed–time profiles in a driving cycle figure. Following the acquiring of the speed vector, it is possible to evaluate the instantaneous power that an engine needs to deliver (P_{eng}, Equation (1)) to overcome the resistance and perform a desired movement.

$$P_{eng} = \frac{1}{\eta_{trans}}\left\{\left[mV\frac{dV}{dt}\right] + \left[k_A(V-W)^2V + C_R mg\, V cos\theta + mg\, V sin\theta\right] + [\beta\mu mgV cos\theta]\right\}, \quad (1)$$

In Equation (1), η_{trans} is the percentage of the engine power that reaches the wheel. The first bracket in the right side of Equation (1) is the inertial power, which is directly influenced by the mass (m), speed (V), and acceleration (dV/dt). The second bracket is the sum of all the resistance powers (aerodynamic drag power, rolling resistance power, and gravitational resistance power), and the third bracket is the braking power. In the aerodynamic drag power, the aerodynamic factor, k_A (i.e., $1/2\rho_{air}AC_D$), considers the fluid specific mass (ρ_{air}), vehicle frontal area (A), vehicle shape coefficient (C_D), and wind speed (W). The rolling resistance power considers the power to deform the tires and dampers and to overcome the vehicle internal friction. It considers the rolling resistance coefficient, C_R, and the inclination of the road, θ. The gravitational resistance power considers the road inclination and the vehicle mass, m. In the braking power (third term in the brackets), β is the braking factor used by the pilot, μ is the friction coefficient between a tire and the road, m is the vehicle mass, g is the gravitational force, and θ is the road inclination. The braking power is null ($\beta = 0$) when $dV/dt \geq 0$ (the vehicle is accelerating), or when it is decelerating, i.e., $dV/dt < 0$. However, the resistance power is sufficient to allow the desired retarding movement. When the resistances are unable to provide

the desired deceleration, the breaking pedal is activated ($\beta > 0$). In this study, all of the simulations considered horizontal roads ($\theta = 0$) and still air ($W = 0$).

$$P_{max,eng}(\Omega) = \begin{cases} C_1\Omega_{min} + C_2\Omega_{min}\left(\Omega_{min} - \Omega_{peak,tor}\right)^2 & \Omega < \Omega_{min} \\ C_1\Omega + C_2\Omega\left(\Omega - \Omega_{peak,tor}\right)^2 & \Omega_{min} \le \Omega \le \Omega_{max} \\ 0 & \Omega > \Omega_{max} \end{cases}, \quad (2)$$

$$C_1 = \frac{P_{max}}{2{\Omega_{peak,pow}}^2}\left(3\Omega_{peak,pow} - \Omega_{peak,tor}\right) \quad (3)$$

$$C_2 = -\frac{P_{max}}{2{\Omega_{peak,pow}}^2\left(\Omega_{peak,pow} - \Omega_{peak,tor}\right)} \quad (4)$$

By definition, the power delivered by an engine (P_{eng}, Equation (1)) is typically lower than the maximum power it can generate at a desired engine speed, Ω ($P_{max,eng}$). In this study, we calculate $P_{max,eng}$ using an empirical correlation described by Ni and Henclewood [34], as expressed in Equation (2). According to it, the curve of $P_{max,eng}$ is a cubic function of the engine speed, and C_1 and C_2 are constants described in the original paper, Equations (3) and (4). These constants are responsible for adjusting the power curve considering the peak power (P_{max}), the engine speed at peak power ($\Omega_{peak,pow}$) and engine speed at peak torque ($\Omega_{peak,tor}$). The engine power is considered constant below the minimum engine speed, Ω_{min}, simulating the clutch usage, and is null above the maximum engine speed, Ω_{max}, simulating the rev limiter.

The relation between the instantaneous engine power (P_{eng}) and the maximum power available by the engine ($P_{max,eng}$) is obtained from the throttle usage, α (0–1), at a particular engine speed.

$$P_{eng} = \alpha P_{max,eng}, \quad (5)$$

It is possible for the power demand obtained by Equation (1) to be higher than the power the engine can actually provide (thus disregarding the inequality, $P_{eng} \le P_{max,eng}$, and the condition, α = [0,1] in Equation (5)). Actually, in that case, the vehicle cannot perform the acceleration required by the cycle, even with $\alpha = 1$. This condition only occurs for low-powered vehicles, such as mopeds, or heavy vehicles when they were not tested in the cycles developed particularly for them.

To calculate the engine efficiency (η_{eng}, Equation (6)) we use the empirical correlation provided by Ben-Chaim et al. [35], considering that η_{eng} is a function of the maximum engine efficiency, η_0, corrected by factors μ_{rev} (Equation (7), considers the engine speed) and μ_{pow} (Equation (8), considers the throttle usage, α, 0–1) under any given speed.

$$\eta_{eng}(\Omega, \alpha) = \eta_0 u_{rev}(\Omega) u_{pow}(\alpha), \quad (6)$$

$$u_{rev}(\Omega) = 0.7107 + 0.9963\left(\frac{\Omega}{\Omega_{peak,pow}}\right) - 1.0582\left(\frac{\Omega}{\Omega_{peak,pow}}\right)^2 + 0.3124\left(\frac{\Omega}{\Omega_{peak,pow}}\right)^3 \quad (7)$$

$$u_{pow}(\alpha) = 0.234 + 1.0592\alpha + 0.8149\alpha^2 - 1.2121\alpha^3 \quad (8)$$

The relation between the engine speed (needed to calculate P_{eng} in Equation (2)) and the vehicle speed, V, is given by the gear geometry and the wheel diameter. With the determination of the delivered power Equations (1)–(5) and the engine efficiency (Equation (6)) variation during the entire driving cycle, it is possible to calculate the vehicle energy consumption per distance traveled:

$$EC = \frac{1}{D}\int_0^t \frac{P_{eng}}{\eta_{eng}} dt, \quad (9)$$

The *FE* can be calculated using the fuel heating value (*FHV*) as follows:

$$FE = \frac{FHV}{EC}, \quad (10)$$

2.4. Characterization of the Reference Vehicle

In this study, to compare all of the cycles, we used the same vehicle for reference. Table 3 lists the parameters of the reference vehicle. In this study, we used the second most sold model in Brazil in 2018, a Hyundai HB20 (hatchback, 1.0 L engine). Some of the vehicle's parameters were obtained from its manual and others were requested to the Brazilian National Institute of Metrology, Standardization and Industrial Quality (INMETRO), responsible for the standard test regarding fuel emission and consumption of all vehicles. This vehicle was chosen because is representative of the Brazilian fleet. In 2018, the hatchback category was the most sold (29%), and the 1.0 L engine displacement was also the most sold category (36% of the total sales) [36]. The peak power, torque, and weight of the reference vehicle is also similar to the other vehicles sold in its category. It should be stressed that Brazilian cars are, on average, lighter and less powerful than American and European cars; and the Brazilian official test fuel is gasohol (E22), a blend of gasoline (78% *v*/*v*) and anhydrous sugarcane ethanol (22% *v*/*v*). For all the energy calculations, for comparison reasons, we consider the same vehicle parameters, engine power curve, and engine efficiency map (Table 3).

Table 3. Engine and vehicle parameters used for the car simulation.

	Parameter	Car
P_{max}	Peak power	55.16 kW
P_{idle}	Idling power	8.0 kW
$\Omega_{peak,pow}$	Engine speed at peak power	6200 rpm
$\Omega_{peak,tor}$	Engine speed at peak torque	4500 rpm
Ω_{min}	Minimum engine speed	900 rpm
η_0	Maximum engine efficiency	22%
η_{trans}	Transmission efficiency	90%
m	Total mass (vehicle + driver)	1126 kg
μ	Tire/road friction coefficient	0.80
k_A	Aerodynamic drag factor	0.428
C_R	Rolling resistance coefficient	0.014
FHV	Fuel heating value	28.99 MJ/liter

3. Results and Discussion

In this section, we first present the original CPs for the 32 reviewed papers, followed by the validation of the extraction and characterization processes. Subsequently, we describe the calculation of the CPs and EPs for the 40 LDCs. Finally, we study the relations between the CPs and the EPs.

3.1. Original Characteristic Parameters for Local Driving Cycles

Table 4 lists the original CPs (CP_{ORIG}) for the 36 LDCs developed for passenger cars, and Table 5 lists CP_{ORIG} for the 41 LDCs for the other vehicle classes (buses, trucks, and motorcycles). The occasional appearance of dashes in both the tables corresponds to the cases in which the authors did not inform the CP value. We emphasize that each author uses a specific formula to calculate the CPs. The last columns of Tables 4 and 5 list the number of local driving cycles (NCs) considered in each paper.

Table 4. Original characteristic kinematic parameter (CP_{ORIG}) for the LDCs for passenger cars (PCs).

Local Driving Cycle	Reference	*V*	*D*	*a*	*d*	*t*	*CT*	*IT*	*AT*	*DT*	*NC*
Athens	[20]	21.2	6.5	0.67	-	1160	-	-	36%	-	1
Bangalore	[11]	16.2	9.4	1.51	−1.76	2088	14%	22%	35%	30%	7
Baqubah	[37]	21.6	6.3	0.24	−0.24	1052	0%	25%	-	-	1
Beijing	[33]	26.1	-	0.51	−0.51	-	15%	13%	36%	37%	11
Beijing	[24]	–	14.5	0.37	−0.40	2536	11%	24%	34%	31%	1
Beijing—Off-peak	[2]	28.8	-	0.51	−0.56	-	39%	24%	19%	18%	2
Beijing—Peak	[2]	23.9	-	0.51	−0.57	-	37%	26%	19%	18%	2
Beijing	[3]	38.5	-	-	-	1200	28%	16%	29%	27%	1
Celje	[14]	25.5	13.0	0.79	−0.84	2453	25%	25%	26%	25%	4
Changchun	[33]	27.8	-	0.56	−0.62	-	12%	19%	36%	33%	11
Chengdu	[33]	31.3	-	0.55	−0.60	-	15%	12%	38%	35%	11
Chennai—Peak	[12]	17.7	5.2	0.45	−0.54	1065	14%	31%	30%	25%	16
Chennai—Off-peak	[12]	22.1	-	0.61	−0.71	-	20%	16%	34%	29%	16
Chongqing	[33]	31.3	-	0.49	−0.56	-	16%	8%	41%	35%	11
Edinburgh	[38]	20	4.2	-	-	835	9%	31%	31%	29%	1
Fortaleza	[23]	23.8	8.4	-	-	1216	0%	43%	30%	27%	1
Hanoi	[13]	19.4	10.0	0.41	−0.38	1862	20%	10%	33%	37%	7
Hefei	[39]	20.2	-	-	-	1237	25%	12%	29%	34%	3
Hong Kong	[32]	15.5	6.3	0.55	−0.59	1471	9%	31%	31%	29%	5
Hong Kong—Urban	[40]	25.0	10.3	0.59	−0.60	1548	12%	18%	35%	34%	3
Hong Kong—Sub Urb	[40]	44.4	18.3	0.56	−0.56	1476	14%	5%	40%	40%	3
Hong Kong—HWY	[40]	38.3	14.9	0.40	−0.41	1401	17%	8%	38%	36%	3
Jilin City	[33]	36.8	-	0.35	−0.50	-	20%	6%	44%	31%	11
Jiutai	[33]	25.5	-	0.37	−0.41	-	20%	5%	39%	36%	11
Mashad	[41]	20.3	-	0.53	−0.54	-	3%	22%	37%	38%	1
Mianyang	[33]	35.3	-	0.48	−0.57	-	15%	12%	40%	33%	11
Nanjing	[42]	30.7	-	0.49	−0.55	-	30%	20%	27%	23%	5
Ningbo	[33]	23.7	-	0.51	−0.58	-	11%	20%	37%	33%	11
Pune	[43]	19.6	-	-	-	1533	56%	18%	14%	11%	1
Santa Maria—5 p.m.	[21]	30.8	11.7	-	-	2017	2%	0%	51%	48%	2
Santa Maria—12 a.m.	[21]	42.9	11.7	-	-	1294	3%	0%	45%	53%	2
Shanghai	[33]	27.6	-	0.55	−0.60	-	9%	26%	34%	31%	11
Sidney	[44]	33.6	5.94	-	-	637	-	18%	-	-	1
Singapore	[19]	32.8	21.5	-	-	2344	26%	21%	29%	25%	1
Tianjin	[33]	22.5	-	0.36	0.43	-	21%	12%	36%	30%	11
Zitong	[33]	32.3	-	0.29	−0.39	-	24%	6%	40%	30%	11
Average		27.2	10.5	0.53	−0.54	1521	17%	17%	34%	31%	8
Standard Deviation		7.5	4.8	0.23	0.33	534	12%	10%	7%	8%	4

Table 4 lists the results for the CPs presented in the original papers (only for the passenger cars). The relatively large standard deviations for the average speed (V = 27.2 ± 7.5 km/h) and acceleration (a = 0.53 ± 0.23 m/s^2) reconfirm numerically that the LDCs worldwide are distinct, thus justifying their differences. In relation to the comparison of the LDCs with SDCs, FTP-75 cycle, and WLTC (class 3) present an average speed of 34.1 km/h and 46.5 km/h, respectively, both being higher than the mean average speed of the LDCs (27.2 km/h).

Comparing the results of the passenger cars and other vehicles, we can see that the mean average speed decreases (Table 4: V = 27.2 ± 7.5 km/h; Table 5: V = 23.3 ± 10.3 km/h) and the acceleration increases (Table 4: a = 0.53 ± 0.23 m/s^2; Table 5: a = 0.56 ± 0.28 m/s^2). To understand these results, we divided Table 5 based on the vehicle category, obtaining a greater speed for trucks (V = 24.3 ± 12.4 km/h), then motorcycles (V = 23.9 ± 8.5 km/h), and then buses (V = 20.6 ± 10.3 km/h). Motorcycles cycles have lower average speeds, probably because trucks cycles have more highway stretches. In terms of acceleration, the higher values were for the motorcycles (a = 0.75 ± 0.27 m/s^2), as expected from their lower masses, followed by those for the trucks (a = 0.38 ± 0.15 m/s^2). There is no acceleration information for buses. Another interesting result is found by analyzing the modes of movement. For trucks, we calculated a very short cruising time (CT = 3% ± 3%), whereas the motorcycles interestingly presented a longer time for the cruising speed (CT = 21% ± 8%); because they are nimble, one would expect motorcycles to spend more time accelerating.

Table 5. CP_{ORIG} for the LDCs for vehicles different from passenger cars: bus (B), motorcycle (M), truck (T).

Local Driving Cycle	Reference	*VT*	*V*	*D*	*a*	*d*	*t*	*CT*	*IT*	*AT*	*DT*	*NC*
Beijing—BRT LS [1]	[27]	B	8.6	2.8	-	-	1167	-	-	-	-	9
Beijing—BRT MS [2]	[27]	B	21.7	7.4	-	-	1220	-	-	-	-	9
Beijing—BRT HS [3]	[27]	B	31.3	10.3	-	-	1185	-	-	-	-	9
Beijing—Express LS [1]	[27]	B	7	2.4	-	-	1226	-	-	-	-	9
Beijing—Express MS [2]	[27]	B	19.5	6.8	-	-	1257	-	-	-	-	9
Beijing—Express HS [3]	[27]	B	35.9	11.3	-	-	1130	-	-	-	-	9
Beijing—Regular LS [1]	[27]	B	8.1	2.7	-	-	1188	-	-	-	-	9
Beijing—Regular MS [2]	[27]	B	19.9	6.0	-	-	1084	-	-	-	-	9
Beijing—Regular HS [3]	[27]	B	30.9	10.9	-	-	1275	-	-	-	-	9
Chennai	[12]	M	22.8	9.1	0.65	−0.73	1448	24%	19%	30%	27%	16
Edinburgh—Urban	[45]	M	33.5	7.3	1.28	−2.59	770	7%	2%	44%	47%	9
Edinburgh—Rural	[45]	M	49.7	9.0	0.89	−0.95	656	8%	1%	45%	46%	9
Hanoi	[13]	M	20.1	11.5	0.42	−0.46	2061	21%	8%	37%	34%	7
Kaohsiung	[18]	M	19.2	4.3	0.66	−0.64	803	24%	24%	25%	26%	5
Kaohsiung	[17]	M	21	6.6	0.58	−0.61	1126	9%	28%	33%	31%	3
Khon Kaen	[46]	M	25.0	8.1	0.64	−0.69	1164	18%	21%	32%	29%	5
Khon Kaen—Electric	[25]	M	22.6	5.0	1.42	−1.05	781	38%	24%	15%	21%	2
Khon Kaen—Gasoline	[25]	M	22.5	4.9	0.64	−0.65	775	19%	27%	28%	26%	2
Pingtung	[18]	M	30.2	6.8	0.69	−0.79	810	22%	10%	36%	32%	5
Shanghai	[31]	B	23	-	0.71	−0.83	-	5%	34%	33%	28%	1
Shanghai—Electric	[26]	M	19.9	9.43	0.50	−0.45	1704	33%	11%	27%	30%	1
Shenyang	[47]	-	28.1	-	0.31	−0.36	-	44%	0%	31%	25%	1
Taichung	[18]	M	18.9	3.8	0.63	−0.61	714	25%	23%	26%	26%	5
Taipei	[22]	M	19.4	5.1	0.80	−0.83	950	19%	20%	32%	30%	1
Taipei	[18]	M	16.6	3.5	0.68	−0.68	763	22%	30%	24%	24%	5
Toronto—HDT [4] Freeway	[1]	T	40.9	-	0.15	−0.28	-	3%	2%	63%	33%	21
Toronto—MDT [5] Freeway	[1]	T	39.7	-	0.14	−0.34	-	1%	2%	69%	28%	21
Toronto—LDT [6] Freeway	[1]	T	52.7	-	0.29	−0.54	-	4%	2%	61%	33%	21
Toronto—LDT [6] M. Artl.	[1]	T	18.4	-	0.58	−0.71	-	3%	17%	44%	36%	21
Toronto—MDT [5] M. Artl.	[1]	T	15.2	-	0.36	−0.65	-	1%	18%	52%	29%	21
Toronto—HDT [4] M. Artl.	[1]	T	16.6	-	0.40	−0.59	-	2%	16%	49%	34%	21
Toronto—HDT [4] LS. Blvd.	[1]	T	28.4	-	0.28	−0.61	-	1%	12%	59%	28%	21
Toronto—MDT [5] LS. Blvd.	[1]	T	25.7	-	0.27	−0.65	-	1%	10%	63%	26%	21
Toronto—LDT [6] LS. Blvd.	[1]	T	34.8	-	0.57	−0.75	-	8%	12%	46%	35%	21
Toronto—HDT [4] U. Ave.	[1]	T	12.4	-	0.40	−0.60	-	1%	22%	46%	31%	21
Toronto—MDT [5] U. Ave.	[1]	T	13.1	-	0.38	−0.63	-	0%	19%	50%	30%	21
Toronto—LDT [6] U. Ave.	[1]	T	13.9	-	0.60	−0.75	-	1%	20%	44%	36%	21
Toronto—HDT [4] Artl Transit	[1]	T	16.9	-	0.41	−0.56	-	6%	19%	43%	32%	21
Toronto—MDT [5] Artl Transit	[1]	T	15.8	-	0.36	−0.59	-	6%	18%	48%	29%	21
Toronto—LDT [6] Artl Transit	[1]	T	19.4	-	0.57	−0.57	-	12%	14%	37%	37%	21
URB	[18]	M	17.4	4.2	0.66	−0.60	877	20%	28%	25%	27%	5
Average			23.3	6.6	0.56	−0.67	1089	13%	16%	41%	31%	13
Standard Deviation			10.3	2.8	0.28	0.42	332	12%	9%	13%	6%	7

[1] Low Speed; [2] Medium Speed; [3] High Speed; [4] Heavy Duty Trucks; [5] Medium Duty Trucks; [6] Light Duty Trucks.

3.2. Validation

The numerical vectors of well-known SDCs for the type—approval tests, such as FTP-75 cycle and WLTC, are easily available online [48,49]. LDC papers typically present only the figure showing the speed as a function of time, whereas the numerical vector is not specified. In addition, they do not generally present all of the CPs considered in this study.

To obtain the CPs from the figures, we used a method comprising two steps: extraction and characterization. The extraction step refers to obtaining the numerical vector from the figure, and the characterization step refers to the process of obtaining the CPs from the extracted numerical vector (ENV). The last step, the simulation, is the process to obtain the EPs from the numerical vector.

Figure 3 presents a flowchart explaining the methodology to obtain the CPs and EPs investigated in this study. In group I, CP_{ORIG} refers to the CPs obtained directly from the papers, as informed by their authors. In group II, the original numerical vector (ONV) is obtained from agencies (in the case of SDCs) or authors (in the case of LDCs). CP_{ONV} refers to our standardized characterization (calculation) of the CPs using the ONV. In Group III, the ENV is the numerical vector we extracted from the figures presented in the papers studied and CP_{ENV} and EP_{ENV} refer to our calculation of the CPs and EPs obtained from the ENV.

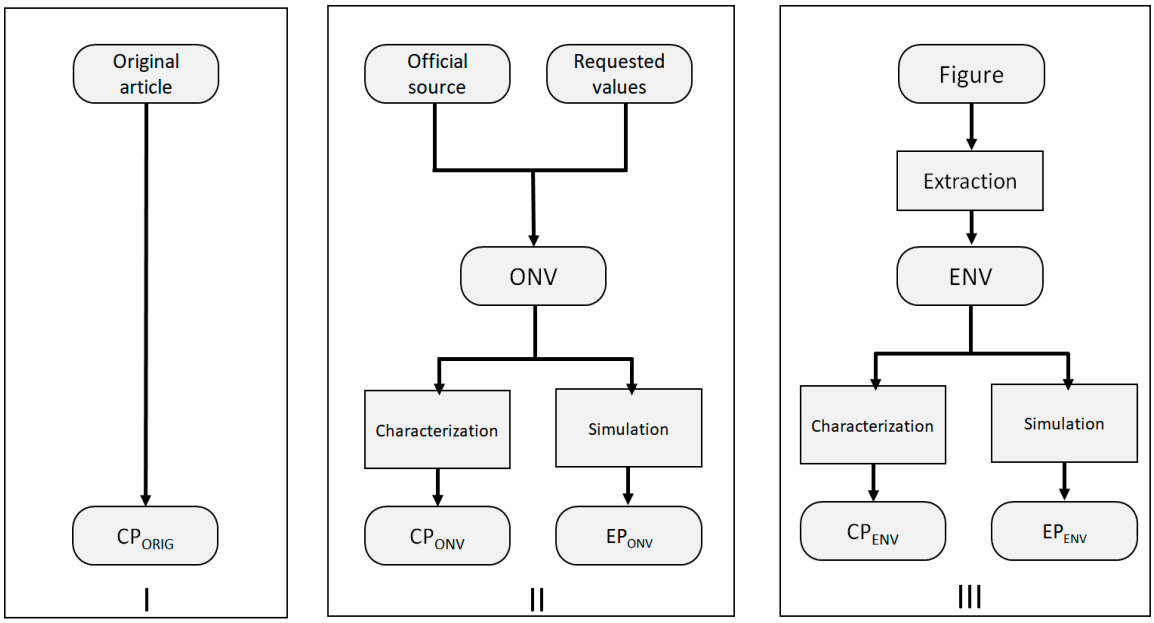

Figure 3. Flowchart explaining the methodology to obtain CPs and energy parameters (Eps).

We used six driving cycles to validate the extraction and characterization methods: two SDCs (FTP-75 cycle and WLTC) and four LDCs (Athens, Toronto, and two from Chennai). The LDC data were obtained directly from the authors. Table 6 contains CP_{ORIG} (as presented by the authors), CP_{ONV} (calculated by us from the ONVs), and CP_{ENV} (calculated by us from the ENVs).

Table 6. Validation Results.

	Driving Cycle		*V*	*D*	*a*	*d*	*t*	*CT*	*IT*	*AT*	*DT*
SDC	FTP-75 cycle	CP_{ORIG}	34.1	17.8	0.51	−0.58	1874	7.7%	17.9%	39.4%	35.0%
		CP_{ONV}	34.1	17.8	0.51	−0.58	1874	7.7%	17.9%	39.4%	35.0%
		CP_{ENV}	34.0	17.7	0.51	−0.59	1874	11.4%	18.6%	37.5%	33.3%
SDC	WLTC (class 3)	CP_{ORIG}	46.5	23.3	0.41	−0.45	1800	3.7%	12.6%	43.8%	39.8%
		CP_{ONV}	46.5	23.3	0.41	−0.45	1800	3.6%	12.6%	43.9%	40.0%
		CP_{ENV}	46.5	23.3	0.44	−0.46	1800	9.8%	13.9%	39.2%	37.0%
LDC	Athens	CP_{ONV}	20.2	6.5	0.71	−0.72	1160	4.1%	27.3%	34.5%	34.1%
		CP_{ENV}	20.0	6.5	0.57	−0.59	1160	5.2%	25.4%	35.4%	34.0%
LDC	Chennai Car Peak	CP_{ONV}	17.7	5.2	0.42	−0.50	1064	7.2%	31.8%	33.4%	27.9%
		CP_{ENV}	17.6	5.2	0.32	−0.50	1065	12.7%	30.0%	34.6%	22.7%
LDC	Chennai Car Off-Peak	CP_{ONV}	22.1	7.9	0.57	−0.67	1292	14.1%	17.0%	37.2%	31.8%
		CP_{ENV}	22.4	8.0	0.37	−0.42	1294	17.4%	16.2%	35.5%	31.0%
LDC	Toronto HDT [1] Freeway	CP_{ONV}	41.0	16.3	0.15	−0.28	1428	2.4%	1.9%	62.8%	32.8%
		CP_{ENV}	40.8	16.2	0.18	−0.25	1430	33.2%	3.0%	37.6%	26.2%

[1] Heavy Duty Trucks.

To validate the characterization step, we compared CP_{ORIG} [50] and CP_{ONV} for FTP-75 cycle and WLTC. From Table 6, we can verify that the characterization is effective, because there is no considerable difference between the values of CP_{ORIG} and CP_{ONV}, for both the SDCs.

To validate the extraction step, CP_{ONV} (calculated from the ONV) is compared to the CP_{ENV} (calculated from the ENV). For FTP-75 cycle, the results for the average speed, distance, time, acceleration, and deceleration were virtually equal. There was a little difference in the time proportion for each driving mode (*CT*, *IT*, *AT*, and *DT*), because the CPs were more sensitive to the acceleration and speed fluctuations. The validation using the WLTC data presented similar results.

For the four LDCs listed in Table 6, we compared CP_{ENV} (characterized following the extraction of the numerical vector from the figure) to CP_{ONV} (from the vectors shared by the authors). For all the cycles, the speed difference was under 0.1 km/h, and the distance difference was shorter than 0.2 km. For the acceleration and deceleration, the difference was less than 0.2 m/s^2. There are some differences between the CP_{ENV} and CP_{ONV} in Table 6, but with little effect on the energy consumption. For example, the relative error for the acceleration in Athens could be considered high (20%). However, the acceleration difference was 0.14 m/s^2, equivalent to a speed variation of 0.5 km/h per second. This is low, because, for example, in the Brazilian law for driving cycle tests, there is a tolerance of 3.2 km/h in relation to the instantaneous velocity, in the type approval test [51]. Therefore, in general, we can deduce that our extraction process is also validated.

3.3. Characteristic Kinematic Parameters from Local Driving Cycles

Table 7 summarizes the results for the CP_{ENV} for 28 LDCs for passenger cars, and Table 8 shows that for the 12 LDCs of other vehicles classes. These CP_{ENV} values were obtained using the methodology described in Figure 4, comprising extraction and characterization.

Table 7. CP_{ENV} of LDCs for passenger cars.

Local Driving Cycle	Reference	*V*	*D*	*a*	*d*	*t*	*CT*	*IT*	*AT*	*DT*
Athens	[20]	20.0	6.5	0.57	−0.59	1160	5%	25%	35%	34%
Bangalore	[11]	16.1	9.3	0.37	−0.49	2088	8%	32%	34%	26%
Beijing	[33]	25.8	7.8	0.44	−0.46	1081	12%	12%	39%	37%
Beijing	[24]	20.4	14.4	0.38	−0.43	2536	14%	27%	31%	28%
Beijing	[3]	34.1	11.3	0.57	−0.71	1192	15%	14%	39%	32%
Changchun	[33]	27.4	8.7	0.51	−0.62	1137	12%	22%	36%	30%
Chengdu	[33]	31.0	10.3	0.48	−0.53	1191	13%	13%	39%	36%
Chennai—Car Peak	[12]	17.6	5.2	0.32	−0.50	1065	13%	30%	35%	23%
Chennai—Car Off-Peak	[12]	22.4	8.0	0.37	−0.42	1294	17%	16%	36%	31%
Chongqing	[33]	31.0	10.0	0.46	−0.49	1157	14%	11%	38%	36%
Edinburgh	[38]	19.7	4.6	0.58	−0.63	835	8%	32%	32%	29%
Fortaleza	[23]	23.7	8.0	0.51	−0.57	1217	8%	30%	33%	29%
Hanoi	[13]	22.1	9.8	0.33	−0.31	1862	18%	14%	33%	34%
Hong Kong	[32]	14.7	6.0	0.46	−0.50	1471	3%	34%	33%	30%
Hong Kong—Urban	[40]	24.0	10.3	0.50	−0.52	1548	14%	22%	33%	32%
Hong Kong—Sub Urb	[40]	44.7	18.3	0.40	−0.40	1475	12%	6%	42%	41%
Hong Kong—HWY	[40]	36.7	14.9	0.28	−0.29	1460	16%	14%	36%	35%
Jilin	[33]	36.3	10.7	0.34	−0.47	1062	17%	7%	44%	32%
Jiutai	[33]	25.4	7.5	0.42	−0.46	1070	15%	5%	42%	38%
Mashad	[41]	19.8	5.6	0.52	−0.50	1019	6%	25%	34%	35%
Mianyang	[33]	35.1	9.9	0.42	−0.60	1017	14%	12%	43%	31%
Nanjing	[42]	36.3	11.8	0.29	−0.35	1174	23%	12%	35%	30%
Ningbo	[33]	23.4	7.4	0.46	−0.51	1137	11%	20%	36%	33%
Santa Maria—12 a.m.	[21]	37.6	13.5	0.20	−0.17	1294	34%	0%	34%	34%
Shanghai	[33]	27.3	8.6	0.50	−0.50	1135	11%	26%	32%	32%
Sydney	[44]	33.6	6.0	0.73	−0.72	637	9%	21%	35%	35%
Tianjin	[33]	22.2	6.6	0.34	−0.42	1075	17%	14%	38%	31%
Zitong	[33]	31.9	8.1	0.28	−0.37	911	21%	8%	41%	31%
Average		27.1	9.2	0.43	−0.48	1261	14%	18%	36%	32%
Standard Deviation		7.6	3.2	0.11	0.12	383	6%	9%	4%	4%
Correlation Coefficient in Relation to Fuel Economy		0.35	0.32	0.81	0.84	0.04	0.90	−0.72	0.13	0.17

For the passenger cars: V_{ENV} = 27.1 ± 7.6 km/h, V_{ORIG} = 28.1 ± 8.0 km/h (considering only the cycles of Table 4 also in Table 7), $V_{FTP\text{-}75}$ = 34.1 km/h, and $V_{WLTC\text{-}3}$ = 46.5 km/h. In relation to acceleration, a_{ENV} = 0.43 ± 0.11 m/s^2, a_{ORIG} = 0.54 ± 0.24 m/s^2 (only for the cycles in both Tables 4 and 7), $a_{FTP\text{-}75}$ = 0.51 m/s^2 and $a_{WLTC\text{-}3}$ = 0.41 m/s^2. The average speed of CP_{ENV} is lower than that of both the SDCs. The average acceleration for CP_{ENV} is similar only to that of WLTC but not to that of

FTP-75 cycle. Table 8 summarizes the 12 LDCs for the motorcycles and the trucks. These cycles are also provided in Table 5 (original values).

Table 8. CP_{ENV} of LDCs for trucks (T) and motorcycles (M).

Local Driving Cycle	Reference	*VT*	*V*	*D*	*a*	*d*	*t*	*CT*	*IT*	*AT*	*DT*
Hanoi	[13]	M	19.9	11.4	0.33	−0.36	2063	26%	10%	33%	31%
Khon Kaen	[46]	M	25.0	8.1	0.51	−0.62	1164	8%	22%	38%	31%
Khon Kaen—Electric	[25]	M	22.9	5.0	0.47	−0.61	781	7%	26%	38%	29%
Khon Kaen—Gasoline	[25]	M	22.6	4.9	0.49	−0.55	775	8%	28%	34%	30%
Shanghai—Electric	[26]	M	19.7	9.3	0.33	−0.32	1704	14%	14%	35%	36%
Taipei	[22]	M	17.5	4.6	0.49	−0.53	950	8%	21%	37%	35%
Toronto—HDT [1] M. Artl.	[1]	T	12.2	6.0	0.40	−0.47	1774	5%	33%	33%	28%
Toronto—HDT [1] Freeway	[1]	T	40.8	16.2	0.18	−0.25	1430	33%	3%	38%	26%
Toronto—LDT [2] M. Artl.	[1]	T	18.1	9.0	0.57	−0.57	1788	6%	33%	30%	30%
Toronto—LDT [2] Freeway	[1]	T	53.1	26.5	0.29	−0.44	1794	23%	3%	44%	29%
Toronto—MDT [3] M. Artl.	[1]	T	15.0	7.5	0.34	−0.53	1795	5%	32%	38%	25%
Toronto—MDT [3] Freeway	[1]	T	39.5	18.9	0.19	−0.24	1723	39%	3%	33%	25%
Average			25.5	10.6	0.38	−0.46	1478	15%	19%	36%	30%
Standard Deviation			12.4	6.7	0.13	0.13	447	12%	12%	4%	3%
Correlation Coefficient in Relation to Fuel Economy			0.27	0.33	−0.65	0.85	0.27	0.76	−0.75	−0.19	0.15

[1] Heavy Duty Trucks; [2] Light Duty Trucks; [3] Medium Duty Trucks.

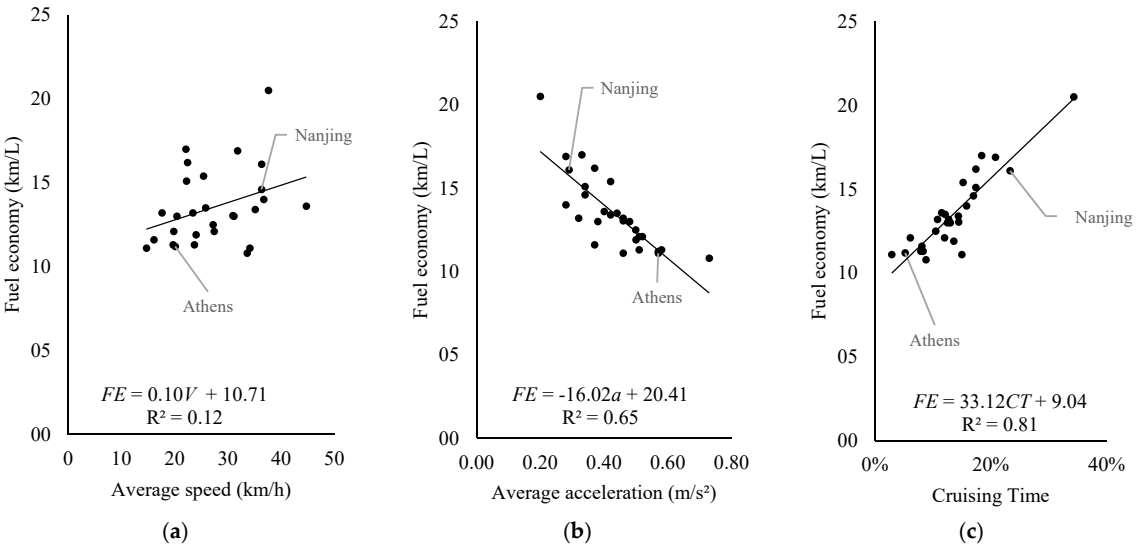

Figure 4. Fuel economy in function of: (**a**) average speed; (**b**) average acceleration; (**c**) cruising time.

3.4. Results for Energy

For comparison purposes, all the EPs for the LDCs (Tables 9 and 10) are calculated for the reference car, defined in Table 3, using Equations (1)–(6). The same car is also used for the LDCs originally developed for motorcycles and trucks (Table 10). The average energy consumption for the passenger cars was EC = 2.1 ± 0.3 MJ/km (FE = 13.5 ± 2.3 km/L, Table 9), whereas for FTP-75 cycle, it was EC = 2.4 MJ/km (FE = 12.0 km/L), and for WLTC was EC = 2.8 MJ/km (FE = 10.5 km/L). In this paper, if not stated otherwise, the economy is expressed in km per liter of E22.

Table 9. EP_{ENV} of the LDCs and SDCs for passenger cars.

Local Driving Cycle	Reference	*FE*	*EC*	*drag*	*inertia*	*rolling*	*idling*
FTP-75 cycle	[48]	12.0	2.4	22%	46%	28%	5%
WLTC (class 3)	[49]	10.5	2.8	38%	36%	25%	2%
Athens	[20]	11.2	2.6	9%	59%	22%	11%
Bangalore	[11]	11.6	2.5	17%	47%	34%	3%
Beijing	[33]	13.5	2.1	15%	53%	30%	2%
Beijing	[24]	13.0	2.2	9%	51%	26%	15%
Beijing	[3]	11.1	2.6	22%	51%	27%	0%
Changchun	[33]	12.1	2.4	25%	32%	39%	3%
Chengdu	[33]	13.0	2.2	16%	53%	30%	0%
Chennai—Car Peak	[12]	13.2	2.2	22%	27%	51%	0%
Chennai—Car Off-Peak	[12]	16.2	1.8	10%	48%	40%	2%
Chongqing	[33]	13.0	2.2	15%	50%	22%	13%
Edinburgh	[38]	11.3	2.6	7%	48%	25%	19%
Fortaleza	[23]	11.3	2.6	10%	51%	23%	16%
Hanoi	[13]	17.0	1.7	7%	45%	37%	11%
Hong Kong	[32]	11.1	2.6	4%	52%	21%	22%
Hong Kong—Urban	[40]	11.9	2.4	17%	45%	30%	8%
Hong Kong—Sub Urb	[40]	13.6	2.1	23%	46%	30%	0%
Hong Kong—HWY	[40]	14.0	2.1	30%	32%	32%	6%
Jilin	[33]	14.6	2.0	17%	47%	34%	3%
Jiutai	[33]	15.4	1.9	8%	58%	33%	2%
Mashad	[41]	12.1	2.4	9%	51%	26%	15%
Mianyang	[33]	13.4	2.2	16%	49%	31%	4%
Nanjing	[42]	16.1	1.8	25%	32%	39%	3%
Ningbo	[33]	13.2	2.2	9%	53%	29%	8%
Santa Maria—12 am	[21]	20.5	1.4	22%	27%	51%	0%
Shanghai	[33]	12.5	2.3	18%	47%	29%	7%
Sydney	[44]	10.8	2.8	15%	50%	22%	13%
Tianjin	[33]	15.1	1.9	14%	45%	36%	5%
Zitong	[33]	16.9	1.7	14%	44%	40%	2%
LDC Average		13.5	2.1	15%	46%	32%	7%
LDC Standard Deviation		2.3	0.3	7%	8%	8%	6%

Table 10. EP_{ENV} of the LDCs for trucks (T) and motorcycles (M).

Local Driving Cycle	Reference	*VT*	*FE*	*EC*	*drag*	*inertia*	*rolling*	*idle*
Khon Kaen	[46]	M	12.2	2.4	11%	56%	27%	6%
Khon Kaen—Electric	[25]	M	12.1	2.4	9%	49%	28%	14%
Khon Kaen—Gasoline	[25]	M	13.1	2.2	10%	51%	28%	11%
Shanghai—Electric	[26]	M	17.8	1.6	7%	42%	39%	10%
Taipei	[22]	M	13.7	2.1	4%	62%	29%	5%
Toronto—HDT [1] Arterial	[1]	T	11.3	2.6	31%	23%	45%	1%
Toronto—HDT [1] Freeway	[1]	T	16.7	1.7	31%	21%	47%	1%
Toronto—LDT [2] Arterial	[1]	T	11.0	2.6	30%	40%	30%	0%
Toronto—LDT [2] Freeway	[1]	T	12.5	2.3	3%	48%	22%	27%
Toronto—MDT [3] Arterial	[1]	T	11.3	2.6	4%	43%	23%	30%
Toronto—MDT [3] Freeway	[1]	T	17.6	1.7	8%	56%	21%	15%
Hanoi	[13]	M	18.1	1.6	6%	44%	44%	6%
Average			13.9	2.2	13%	44%	32%	10%
Standard Deviation			2.8	0.4	11%	12%	9%	10%

[1] Heavy Duty Trucks; [2] Light Duty Trucks; [3] Medium Duty Trucks.

In Table 9, EC is the energy consumption of the whole cycle, in MJ/km, comprising all the modes of energy (drag, inertia, rolling, and idling). It is important to emphasize that these values are in MJ of the fuel, and already consider the engine and transmission efficiency. The gravitational force is not included, because we simulated the reference vehicle considering a plain road, and the wind speed was 0 km/h. Comparing the average values of the LDCs in Table 9 with those with FTP-75 cycle and WLTC, we see that WLTC has a higher drag power (LDCs average: 0.3 MJ/km; WLTC: 1.1 MJ/km; FTP-75 cycle: 0.5 MJ/km) owing to its higher speed. In comparison, FTP-75 cycle has the higher inertial power (LDCs average: 1.0 MJ/km; WLTC: 1.0 MJ/km; FTP-75 cycle: 1.1 MJ/km), owing to its higher acceleration.

In Table 9, on average, the highest energy spent during a driving cycle is to overcome the inertia (46%), followed by for the rolling resistance (32%), aerodynamic drag (15%), and idling (7%). The drag is not extremely important, owing to the low average speed. Focusing on specific driving cycles, WLTC has a high drag energy percentage (38%), owing to its high speed, whereas Hong Kong has a low drag (4%), owing to its low speed. Athens has a high inertial energy percentage (59%), owing to its high acceleration allied to low speed, and Hong Kong has a high idling energy percentage (22%), because it has a long idling time. WLTC has a high (2.8 MJ/km) overall fuel energy, owing to its high speed, whereas Santa Maria has a low value (1.4 MJ/km), owing to its low acceleration.

From Table 9, it also possible to obtain an estimation of the CO_2 emitted using stoichiometric calculation. The energy consumption (MJ/km) can be converted to CO_2 emitted when multiplying it by a factor of 0.072 kg CO_2/MJ of E22.

Table 10 summarizes the energy splitting considering the cycles developed for other vehicles (trucks and motorcycles). We emphasize that although the cycles are developed for distinct vehicles, for comparison, all of the energy calculations were conducted for the same reference vehicle (Table 3). In fact, in these calculations, the differences in the masses of the motorcycles and the trucks were not considered (our aim here was to compare cycles, not vehicles). The cycles developed for motorcycles (simulated with the reference car) present lower energy consumption (2.1 MJ/km), owing to their lower speed (21.3 km/h), and for trucks (also simulated with the reference car), the values are 2.3 MJ/km and 29.8 km/h. The inertial resistance percentage is higher for the cycles developed for motorcycles (50%), because of their higher acceleration (0.44 m/s^2), than that for the cycles for trucks (38%; a = 0.33 m/s^2). For comparison, by changing the characteristics of the vehicles (e.g., drag, mass, and power peak), if we simulated FTP-75 cycle with a motorcycle, then we would obtain FE = 32.1 km/L (E22) and EC = 0.9 MJ/kg; and for a truck, FE = 3.7 km/L (diesel) and EC = 9.6 MJ/kg.

The simulations provided in Table 9 (cycles for the passenger cars) point to the gains one could obtain with each technological improvement. The major consumption is by the inertial resistance (46%), thus the improvement should point primarily to mass reduction. One should remember (Equation (1)) that the mass also influences the rolling and gravitational resistances; thus, mass gains would have a higher impact than only reducing the inertial resistance. The second major consumption is by the rolling resistance (32%), which can be decreased with a higher tire pressure, stiffer dampers, and lowering the mass. However, such ameliorations do not depend only on the vehicle itself, because they depend on the quality of the roads as well. The aerodynamic drag is not extremely important (15%) owing to the lower speeds (recalling that aerodynamic improvements in general increase the price of a vehicles). The use of a start–stop strategy could decrease the energy consumed during idling (7%). Our simulations did not consider the road inclination, because the cycles did not yield this variable. However, certainly the gravitational resistance is also a major factor in energy consumption.

Indeed, the general recommendations continue to be valid, e.g., the adoption of hybrid and electric vehicles and regenerative braking. These modifications can be considered in the reference vehicle/engine model of this study, changing the total mass and maximal engine efficiency of the vehicle in Table 3. Table 11 summarizes the values of the EC and FE in the case of technology improvements or under other road conditions. For example, if the car mass was to be reduced by 50%, the energy consumption would decrease by 17%. The use of ethanol as a fuel instead of E22 would decrease the energy consumption in 2% (owing to its higher-octane number, compression ratio, and engine

efficiency). The effect of the wind is small (4% for a 5 km/h wind). A slope of 2° would increase the energy consumption by 72%, from 2.39 to 4.11 MJ/km. With road inclination, 43% of the energy is spent to overcome the gravitational resistance, whereas drag, inertia, rolling, and idle contributes with 14%, 21%, 19%, and 3%, respectively.

Table 11. Energy consumption variation for simulation changes for FTP-75 cycle.

Cases	*EC* (MJ/km)	Variation of *EC*	*FE* (km/L)
Standard	2.39		12.1
$\frac{1}{2}$ m	1.98	−17%	14.7
$\frac{1}{2}$ C_R	2.06	−14%	14.1
$\frac{1}{2}$ k_A	2.11	−12%	13.8
$\frac{1}{2}$ P_{max_eng}	2.08	−13%	13.9
2 P_{max_eng}	2.40	0%	12.1
Ethanol	2.35	−2%	8.6
$\theta = 2°$	4.11	72%	7.05
$W = 5$ km/h	2.49	4%	11.7

Returning to Table 7 (the LDCs developed for cars), the last row presents the correlation between the *FE* and the CPs. For cars, the highest correlation was for the cruising time ($r = 0.90$), followed by for deceleration ($r = 0.84$) and acceleration ($r = -0.81$). It might seem surprising to find the cruising time as the most important factor influencing the *FE*, because according to Table 9, inertia (thus acceleration) is the most important energy fraction in the consumption. The explanation is that there is a correlation between the cruising time and the acceleration ($r = -0.71$): the longer the cruising time (constant speed), the lower the acceleration. There is also a strong correlation between the deceleration and the acceleration ($r = -0.89$), because each time a car brakes, it has to subsequently accelerate, which also explains the influence of deceleration on the *FE*. Unexpectedly, there is no correlation between the time percentage a car accelerates and its energy consumption; this occurs because there is no correlation between a and AT ($r = -0.11$).

No good correlation is found between the *FE* and the average speed of the car ($r = 0.35$); therefore, it is possible to conclude that the average speed is not a good alternative to estimate fuel economy. This conclusion is similar to that of Ho et al. [19]. Obviously, in general, the energy consumption varies with the average speed, because the drag energy varies with V^3. We did not find this correlation because the average speed for the studied LDCs (for cars) was low, 27.1 (±7.6) km/h. This is listed in Table 9, in which only 15% of the energy is owing to the aerodynamic drag.

Figure 4 illustrates the variation of the *FE* with the average speed (Figure 4a), average acceleration (Figure 4b), and cruising time (Figure 4c), illustrating the correlation coefficients (r) discussed above. Equation (11) provides a good estimation of the *FE* using only the CPs, without the necessity of simulating the car as conducted in this study. The mean deviation of Equation (11) is ±0.7 km/L (i.e., 6% of the average *FE*)

$$FE = 33.12\ CT + 9.04, \quad (11)$$

Recalling, all the calculations until now were conducted for a 1 ton car. For example, if the car was 1.4 ton, the *FE* would be decreased by 2.7 km/L.

To understand the importance of acceleration (or cruising time) for the energy consumption (or *FE*), we chose two cycles from Figure 4 with distinct values of the *FE*: Athens and Nanjing. Both were selected because they were in the main cluster of Figure 4c and near the regression curve. From the data for Athens ($V = 20.1$ km/h, $a = 0.57$ m/s^2, $FE = 11.2$ km/L, $EC = 2.6$ MJ/km, $CT = 5\%$, $D = 6.5$ km, $t = 1160$ s) and Nanjing ($V = 36.3$ km/h, $a = 0.29$ m/s^2, $FE = 16.1$ km/L, $EC = 1.8$ MJ/km, $CT = 23\%$, $D = 11.8$ km, $t = 1174$ s), we again confirm that acceleration (reflected in cruising time, *CT*, as discussed above) is the main parameter influencing the energy consumption.

Figure 5a presents the speed vectors of the two cities (Athens and Nanjing), from which it is noticeable that in Nanjing, the average speed is higher than in Athens. Figure 5b presents the evolution of the energy consumption (accumulated energy per total cycle distance, MJ/km) for both the cycles. Figure 5c displays the traveled distances for both the cities (it should be noted that the Athens cycle is half the distance of Nanjing, although requiring approximately the same total time).

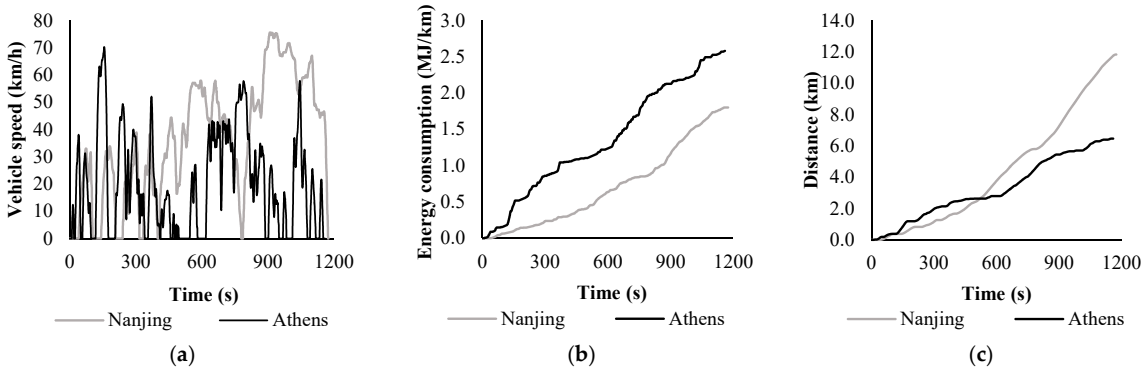

Figure 5. For Athens LDC and Nanjing LDC: (**a**) vehicle speed, (**b**) energy consumption, and (**c**) distance, in function of time.

By analyzing the energy simulations for the LDCs in Table 9 (passenger car), we calculated that 75% of the energy consumption (when the car is accelerating) occurs with accelerations under 38% of the maximal acceleration of each cycle. Approximately $\frac{1}{4}$ of the total consumption occurs when the acceleration is in each of the ranges of 0–11%, 12–21%, 22–38%, and 39–100% of the maximum acceleration of the vehicle. Returning to Equation (1), we note that inertia contributes with a term aV; therefore, higher accelerations should be expected to be more important than lower accelerations, for the energy consumption. However, lower accelerations, regardless of their lower values, are more frequent in the cycles (median acceleration of the cycles is 0.31 m/s^2 and the mean acceleration is 0.44 m/s^2), contributing more to the energy consumption in the integral of Equation (5) than the higher accelerations.

4. Conclusions

In this study, we organized 77 local driving cycles (LDCs, Tables 4 and 5) from 32 papers, collecting their main kinematic parameters (e.g., average speed, acceleration, and idling percentage). It was possible to extract (using a method validated in this paper, Table 6) 40 numerical vectors from the speed–time profiles in the 20 papers, which were organized into two tables: 28 LDCs developed for cars (Table 7) and 12 LDCs developed for motorcycles and trucks (Table 8). In those tables (Tables 6–8), the kinematic parameters were re-calculated using a standardized procedure. Subsequently, we simulated the energy consumption for each LDC, dividing the energy into inertia, drag, rolling, and idling (Tables 9 and 10). Finally, we analyzed the influence of the kinematic parameters on the fuel economy (correlations shown in the bottom of Tables 7 and 8) and the effect of the parameters of the vehicle (Table 11) on the energy consumption and fuel economy.

We can now proceed with the conclusion, emphasizing that the main objective of this study is to numerically compare LDCs among themselves and against SDCs. Based on our results, we can numerically affirm that there are significant differences between LDCs and SDCs as the following results demonstrate: LDCs have lower average speed and acceleration (V = 27.1 km/h, a = 0.43 m/s^2) when compared to one of the most prominent SDCs worldwide, FTP-75 cycle (V = 34.1 km/h, a = 0.51 m/s^2). In this study, we found (as partially expected) acceleration as the most important factor for energy consumption. The studied LDCs have relatively low average speed (14.7 to 44.7 km/h, Table 7); therefore, we could not obtain a correlation between the average speed and the energy consumption. However, this does not suggest that there is no such correlation in general.

For the cycles investigated in this study, the average use of energy was 46% for inertia, 32% for rolling, 15% for drag, and 7% for idling. Therefore, the most important technological improvement of the vehicles should be mass reduction (besides the improvement of engine technologies, e.g., the use of hybrids or electrical propulsion). In addition to inertia, decreasing the mass also presented an impact on the rolling and gravitational resistances (Equation (1)). We highlight that the qualitative results can be used for a general comparison of the cycles, but the numeric results apply only for the reference car informed in Table 3.

We found a strong correlation existed between the average acceleration, cruising time, and average deceleration and between these parameters and the fuel economy. We developed a numerical correlation between the *FE* (fuel economy) and *CT* (cruising time), which permits the estimation of the fuel economy of a cycle without the energy simulations discussed in this paper. The fuel economy was observed to be strongly influenced by the acceleration (correlation $r = -0.81$). For example, in the limit cases in Tables 7 and 9, Santa Maria ($a = 0.20$ m/s^2; $FE = 20.5$ km/L) presented a higher fuel economy than Sydney ($a = 0.73$ m/s^2; $FE = 10.8$ km/L).

Table 9 demonstrates that there are significant differences in the LDCs in relation to the energy use. For example, the use of the fuel energy to overcome inertia varies in the range of 0.4–1.5 MJ/km, rolling 0.5–1.1 MJ/km, aerodynamic drag 0.1–0.6 MJ/km, and idling 0.0–0.6 MJ/km (these results could be obtained by multiplying the percentages by *EC* in Table 9).

SDCs are important to compare the impacts of different technologies on the energy consumption and emissions in different countries, whereas local driving cycles assess these parameters for a specific region. We calculated that the LDCs evaluated in this study significantly differ among themselves. For cars, the standard deviation of the acceleration in the LDCs is 0.11 m/s^2 and in speed is 7.6 km/h, resulting in a standard deviation in fuel economy of 2.3 km/L. For other vehicles, the standard deviation in fuel economy is 2.8 km/L. When the average results of the LDCs for passenger cars are compared to the SDCs, they present a difference in the fuel economy of 12.5% (1.5 km/L) and of 28.6% (3.0 km/L) when compared to FTP-75 cycle and WLTC-3, respectively. Therefore, this paper confirms the reasoning of the worldwide praxis of developing local driving cycles. The numerical results we obtained show that the SDCs might not be representative of specific regions, so they should not be used as the solely legal testing procedure. We suggest that countries and major cities consider developing their own LDCs, in addition to SDCs, to better evaluate their reality.

Author Contributions: Conceptualization, G.M.S.d.A., F.W.C.d.A. and F.S.M.; methodology, G.M.S.d.A., M.P.M.d.N.S. and F.W.C.d.A.; software, G.M.S.d.A.; validation, M.P.M.d.N.S.; formal analysis, F.W.C.d.A., data curation, G.M.S.d.A. and M.P.M.d.N.S.; writing—original draft, F.W.C.d.A.; Writing—review and editing, G.M.S.d.A., M.P.M.d.N.S. and F.S.M.; supervision, F.S.M. All authors have read and agreed to the published version of the manuscript.

Funding: This study was financed in part by the Coordenação de Aperfeiçoamento de Pessoal de Nível Superior—Brasil (CAPES)—Finance Code 001.

Acknowledgments: The authors would like to thank the authors who kindly shared their research data with us (Srinath Mahesh—Chennai, Evangelos Tzirakis—Athens, Matthew Roorda and Glareh Amirjamshidi—Toronto). The authors also thank UFPE, CAPES and PROAP-CAPES for their financial support.

Conflicts of Interest: The authors declared no potential conflicts of interest with respect to the research, authorship, and/or publication of this article.

References

1. Amirjamshidi, G.; Roorda, M.J. Development of simulated driving cycles for light, medium, and heavy duty trucks: Case of the Toronto Waterfront Area. *Transp. Res. Part. D Transp. Environ.* **2015**, *34*, 255–266. [CrossRef]
2. Ma, R.; He, X.; Zheng, Y.; Zhou, B.; Lu, S.; Wu, Y. Real-world driving cycles and energy consumption informed by large-sized vehicle trajectory data. *J. Clean. Prod.* **2019**, *223*, 564–574. [CrossRef]
3. Wang, Z.; Zhang, J.; Liu, P.; Qu, C.; Li, X. Driving Cycle Construction for Electric Vehicles Based on Markov Chain and Monte Carlo Method: A Case Study in Beijing. *Energy Procedia* **2019**, *158*, 2494–2499. [CrossRef]

4. Al-Samari, A. Study of emissions and fuel economy for parallel hybrid versus conventional vehicles on real world and standard driving cycles. *Alex. Eng. J.* **2017**, *56*, 721–726. [CrossRef]
5. Cubito, C.; Millo, F.; Boccardo, G.; Di Pierro, G.; Ciuffo, B.; Fontaras, G.; Serra, S.; Garcia, M.O.; Trentadue, G. Impact of Different Driving Cycles and Operating Conditions on CO_2 Emissions and Energy Management Strategies of a Euro-6 Hybrid Electric Vehicle. *Energies* **2017**, *10*, 1590. [CrossRef]
6. Montazeri-Gh, M.; Mahmoodi-k, M. Development a new power management strategy for power split hybrid electric vehicles. *Transp. Res. Part. D Transp. Environ.* **2015**, *37*, 79–96. [CrossRef]
7. Montazeri-Gh, M.M.-K. Optimized predictive energy management of plug-in hybrid electric vehicle based on traffic condition. *J. Clean. Prod.* **2016**, *139*, 935–948. [CrossRef]
8. Huertas, J.I.; Quirama, L.F.; Giraldo, M.; Díaz, J. Comparison of three methods for constructing real driving cycles. *Energies* **2019**, *12*, 665. [CrossRef]
9. Fontaras, G.; Zacharof, N.-G.; Ciuffo, B. Fuel consumption and CO_2 emissions from passenger cars in Europe—Laboratory versus real-world emissions. *Prog. Energy Combust. Sci.* **2017**, *60*, 97–131. [CrossRef]
10. Lim, J.; Lee, Y.; Kim, K.; Lee, J. Experimental Analysis of Calculation of Fuel Consumption Rate by On-Road Mileage in a 2.0 L Gasoline-Fueled Passenger Vehicle. *Appl. Sci.* **2018**, *8*, 2390. [CrossRef]
11. Mayakuntla, S.K.; Verma, A. A novel methodology for construction of driving cycles for Indian cities. *Transp. Res. Part. D Transp. Environ.* **2018**, *65*, 725–735. [CrossRef]
12. Arun, N.H.; Mahesh, S.; Ramadurai, G.; Shiva Nagendra, S.M. Development of driving cycles for passenger cars and motorcycles in Chennai, India. *Sustain. Cities Soc.* **2017**, *32*, 508–512. [CrossRef]
13. Tong, H.Y.; Tung, H.D.; Hung, W.T.; Nguyen, H.V. Development of driving cycles for motorcycles and light-duty vehicles in Vietnam. *Atmos. Environ.* **2011**, *45*, 5191–5199. [CrossRef]
14. Knez, M.; Muneer, T.; Jereb, B.; Cullinane, K. The estimation of a driving cycle for Celje and a comparison to other European cities. *Sustain. Cities Soc.* **2014**, *11*, 56–60. [CrossRef]
15. Barlow, T.J.; Latham, S.; McCrae, I.S.; Boulter, P.G. *A Reference Book of Driving Cycles for Use in the Measurement of Road Vehicle Emissions*; TRL: Berks, UK, 2009; ISBN 978-1-84608-924-4.
16. Giakoumis, E.G. *Driving and Engine Cycles*; Springer: Berlin/Heidelberg, Germany, 2016; ISBN 978-3-319-49034-2.
17. Tsai, J.H.; Chiang, H.L.; Hsu, Y.C.; Peng, B.J.; Hung, R.F. Development of a local real world driving cycle for motorcycles for emission factor measurements. *Atmos. Environ.* **2005**, *39*, 6631–6641. [CrossRef]
18. Chen, K.S.; Wang, W.C.; Chen, H.M.; Lin, C.F.; Hsu, H.C.; Kao, J.H.; Hu, M.T. Motorcycle emissions and fuel consumption in urban and rural driving conditions. *Sci. Total Environ.* **2003**, *312*, 113–122. [CrossRef]
19. Ho, S.H.; Wong, Y.D.; Chang, V.W.C. Developing Singapore Driving Cycle for passenger cars to estimate fuel consumption and vehicular emissions. *Atmos. Environ.* **2014**, *97*, 353–362. [CrossRef]
20. Karavalakis, G.; Tzirakis, E.; Zannikos, F.; Stournas, S.; Bakeas, E.; Arapaki, N.; Spanos, A. Diesel/soy methyl ester blends emissions profile from a passenger vehicle operated on the European and the athens driving cycles. *SAE Tech. Pap. Ser.* **2007**. [CrossRef]
21. Roso, V.R.; Martins, M.E.S. Evaluation of a Real-World Driving Cycle and its Impacts on Fuel Consumption and Emissions. *SAE Tech. Pap. Ser.* **2015**, *1*. [CrossRef]
22. Tzeng, G.-H.; Chen, J.-J. Developing a Taipei Motorcycle Driving Cycle for Emissions and Fuel Economy. *Transp. Res. Part. D Transp. Environ.* **1998**, *3*, 19–27. [CrossRef]
23. Azevedo, J.A.H.; Cassiano, D.R.; Feitosa, B.B.; De Oliveira, M.L.M.; Lima, E.P.; Bertoncini, B.V. Influências dos modos de operação nas emissões de poluentes provenientes de veículos flex em região urbana. *Transportes* **2017**, *25*, 91. [CrossRef]
24. Gong, H.; Zou, Y.; Yang, Q.; Fan, J.; Sun, F.; Goehlich, D. Generation of a driving cycle for battery electric vehiclesA case study of Beijing. *Energy* **2018**, *150*, 901–912. [CrossRef]
25. Koossalapeerom, T.; Satiennam, T.; Satiennam, W.; Leelapatra, W.; Seedam, A.; Rakpukdee, T. Comparative study of real-world driving cycles, energy consumption, and CO_2 emissions of electric and gasoline motorcycles driving in a congested urban corridor. *Sustain. Cities Soc.* **2019**, *45*, 619–627. [CrossRef]
26. Rechkemmer, S.K.; Zang, X.; Boronka, A.; Zhang, W.; Sawodny, O. Utilization of Smartphone Data for Driving Cycle Synthesis Based on Electric Two-Wheelers in Shanghai. *IEEE Trans. Intell. Transp. Syst.* **2020**. [CrossRef]
27. Lai, J.; Yu, L.; Song, G.; Guo, P.; Chen, X. Development of City-Specific Driving Cycles for Transit Buses Based on VSP Distributions: Case of Beijing. *J. Transp. Eng.* **2013**, *139*, 749–757. [CrossRef]

28. Selph, S.; Ginsburg, A.D.; Chou, R. Impact of contacting study authors to obtain additional data for systematic reviews: Diagnostic accuracy studies for hepatic fibrosis. *Syst. Rev.* **2014**, *3*. [CrossRef] [PubMed]
29. Burda, B.U.; O'Connor, E.A.; Webber, E.M.; Redmond, N.; Perdue, L.A. Estimating data from figures with a Web-based program: Considerations for a systematic review. *Res. Synth. Methods* **2017**, *8*, 258–262. [CrossRef]
30. Kadic, A.J.; Vucic, K.; Dosenovic, S.; Sapunar, D.; Puljak, L. Extracting data from figures with software was faster, with higher interrater reliability than manual extraction. *J. Clin. Epidemiol.* **2016**, *74*, 119–123. [CrossRef]
31. Shen, P.; Zhao, Z.; Li, J.; Zhan, X. Development of a typical driving cycle for an intra-city hybrid electric bus with a fixed route. *Transp. Res. Part. D Transp. Environ.* **2018**, *59*, 346–360. [CrossRef]
32. Tong, H.Y.; Hung, W.T.; Cheung, C.S. Development of a driving cycle for Hong Kong. *Atmos. Environ.* **1999**, *33*, 2323–2335. [CrossRef]
33. Wang, Q.; Huo, H.; He, K.; Yao, Z.; Zhang, Q. Characterization of vehicle driving patterns and development of driving cycles in Chinese cities. *Transp. Res. Part. D Transp. Environ.* **2008**, *13*, 289–297. [CrossRef]
34. Ni, D.; Henclewood, D. Simple engine models for VII-enabled in-vehicle applications. *IEEE Trans. Veh. Technol.* **2008**, *57*, 2695–2702. [CrossRef]
35. Ben-Chaim, M.; Shmerling, E.; Kuperman, A. Analytic modeling of vehicle fuel consumption. *Energies* **2013**, *6*, 117–127. [CrossRef]
36. FENABRAVE Emplacamentos: Veículos Novos 2018. Available online: http://www.fenabrave.org.br/Portal/conteudo/emplacamentos (accessed on 15 October 2020).
37. Al-Samari, A. Real-World Driving Cycle: Case Study of Baqubah, Iraq. *Diyala J. Eng. Sci.* **2017**, *10*, 39–47. [CrossRef]
38. Esteves-Booth, A.; Muneer, T.; Kirby, H.; Kubie, J.; Hunter, J. The measurement of vehicular driving cycle within the city of Edinburgh. *Transp. Res. Part. D Transp. Environ.* **2001**, *6*, 209–220. [CrossRef]
39. Liu, B.; Shi, Q.; He, L.; Qiu, D. A study on the construction of Hefei urban driving cycle for passenger vehicle. *IFAC PapersOnLine* **2018**, *51*, 854–858. [CrossRef]
40. Hung, W.T.; Tong, H.Y.; Lee, C.P.; Ha, K.; Pao, L.Y. Development of a practical driving cycle construction methodology: A case study in Hong Kong. *Transp. Res. Part. D Transp. Environ.* **2007**, *12*, 115–128. [CrossRef]
41. Pouresmaeili, M.A.; Aghayan, I.; Taghizadeh, S.A. Development of Mashhad driving cycle for passenger car to model vehicle exhaust emissions calibrated using on-board measurements. *Sustain. Cities Soc.* **2018**, *36*, 12–20. [CrossRef]
42. Yang, Y.; Li, T.; Hu, H.; Zhang, T.; Cai, X.; Chen, S.; Qiao, F. Development and emissions performance analysis of local driving cycle for small-sized passenger cars in Nanjing, China. *Atmos. Pollut. Res.* **2019**. [CrossRef]
43. Kamble, S.H.; Mathew, T.V.; Sharma, G.K. Development of real-world driving cycle: Case study of Pune, India. *Transp. Res. Part. D Transp. Environ.* **2009**, *14*, 132–140. [CrossRef]
44. Kent, J.H.; Allen, G.H.; Rule, G. A driving cycle for Sydney. *Transp. Res.* **1978**, *12*, 147–152. [CrossRef]
45. Saleh, W.; Kumar, R.; Kirby, H.; Kumar, P. Real world driving cycle for motorcycles in Edinburgh. *Transp. Res. Part. D Transp. Environ.* **2009**, *14*, 326–333. [CrossRef]
46. Seedam, A.; Satiennam, T.; Radpukdee, T.; Satiennam, W. Development of an onboard system to measure the on-road driving pattern for developing motorcycle driving cycle in Khon Kaen city, Thailand. *IATSS Res.* **2015**. [CrossRef]
47. Yang, Y.; Zhang, Q.; Wang, Z.; Chen, Z.; Cai, X. Markov chain-based approach of the driving cycle development for electric vehicle application. *Energy Procedia* **2018**, *152*, 502–507. [CrossRef]
48. EPA Vehicle and Fuel Emissions Testing. Available online: https://www.epa.gov/vehicle-and-fuel-emissions-testing/dynamometer-drive-schedules (accessed on 15 August 2020).
49. Tutuianu, M.; Marotta, A.; Steven, H.; Ericsson, E.; Haniu, T.; Ichikawa, N.; Ishii, H. Development of a World-Wide Worldwide Harmonized Light Duty Driving Test Cycle. 2013. Available online: http://www.unece.org.net4all.ch/fileadmin/DAM/trans/doc/2014/wp29grpe/GRPE-68-03e.pdf (accessed on 15 August 2020).

50. Kühlwein, J.; German, J.; Bandivadekar, A. *Development of Test. Cycle Conversion Factors among Worldwide Light Duty Vehicle CO_2 Emission Standards*; International Council on Clean Transportation: Washington, DC, USA, 2014; Available online: http://www.theicct.org/sites/default/files/publications/ICCT_LDV-test-cycle-conversion-factors_sept2014.pdf (accessed on 15 August 2020).
51. Associação Brasileira de Normas Técnicas (ABNT). *NBR 6601 Light Road Vehicles—Determination of Hydrocarbon, Carbon Monoxide, Nitrogen Oxide, Carbon Dioxide and Particulate Material on Exhaust Gas*; Associação Brasileira de Normas Técnicas: São Paulo, Brazil, 2012.